Lehigh University
Lehigh Preserve

Fritz Laboratory Reports   Civil and Environmental Engineering

1970

Web buckling strength of beam-to-column connections, September 1970 (74-1) PB 234 621/AS

W. F. Chen

I. J. Oppenheim

Follow this and additional works at: http://preserve.lehigh.edu/engr-civil-environmental-fritz-lab-reports

333.10

LEHIGH UNIVERSITY
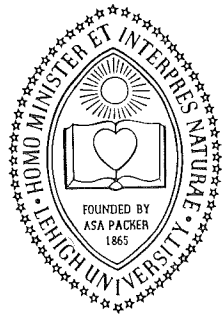
Beam-to-Column Connections

WEB BUCKLING STRENGTH OF

BEAM-TO-COLUMN CONNECTIONS

by

W. F. Chen

I. J. Oppenheim

September 1970

Fritz Engineering Laboratory Report No. 333.10

Beam-to-Column Connections

WEB BUCKLING STRENGTH
OF BEAM-TO-COLUMN CONNECTIONS

by

W. F. Chen

and

I. J. Oppenheim

Department of Civil Engineering

Fritz Engineering Laboratory
Lehigh University
Bethlehem, Pennsylvania

September 1970

Fritz Engineering Laboratory Report No. 333.10

TABLE OF CONTENTS

WEB BUCKLING STRENGTH OF
BEAM-TO-COLUMN CONNCETIONS

by

W. F. Chen[1]

and

I. J. Oppenheim[2]

ABSTRACT

In the design of an interior beam-to-column connection, consideration must be given to column web stiffening. Stiffening may be required to increase the column web shear capacity or stiffen the column web opposite the beam compression or tension flange.

This report is an examination of the criteria for stiffening the column web opposite the beam compression flange(s). This compression region is simulated in a manner allowing rapid and easy testing of specimens. The two most important variables in the study are the yield strength and the web depth-to-web thickness ratio. It is found that the formulas given in the present AISC Specification are conservative, especially for structural carbon steels.

[1]Assistant Professor of Civil Engineering, Fritz Engineering Laboratory, Lehigh University, Bethlehem, Pennsylvania.

[2]Graduate Student, Fritz William College, Cambridge University, England. Formerly Teaching Assistant, Department of Civil Engineering, Lehigh University, Bethlehem, Pennsylvania.

1. INTRODUCTION

1.1 Purpose

In the present AISC Specification (February,
1969 [1]) there are two formulas governing the require-
ments for stiffening the compression region of an
interior beam-to-column connection. Formula (1.15-1)
(or ASCE Manual No. 41, Eq. 8.21, Ref. 2) gives the
strength a column web will develop in resisting the
compression forces delivered by beam flanges. It has
the form (see Fig. 1 and Nomenclature)

$$w < \frac{C_1 A_f}{t_b + 5k} \tag{1}$$

The application of this formula is limited
to cases where the column web depth-to-thickness ratio
is small enough to preclued instability. The limiting
ratio is described by Formula (1.15-2)*

$$w \leq \frac{\sqrt{\sigma_y}\ d_c}{180} \tag{2}$$

The second formula, and the instability effect,
have not been completely examined. The purpose of this
report is to study this effect, including its application
to columns of high-strength steel. A series of tests
were performed to accomplish this.

---

*Some printings of the Specification have $w \leq \dfrac{d_c}{5\sqrt{\sigma_y}}$ which
is an error. It should be as given here.

1.2 Previous Work

A program of research undertaken at Lehigh University in the late 1950's is the basis for many of the current design provisions for beam-column connections [1]. In that work the strength of the compression region was studied but not its stability. Furthermore, all the specimens were of steel with a 36 ksi yield point. Their simulation of the compression region of the column web as shown in Fig. 1 is the one used in this current study.

The stress distribution over a width of $t_b + 5k$ is based on a curve fit to an elastic solution by Parkes. This is described in the appendix to the Fritz Lab. report of Graham et al [3].

2. THEORETICAL ANALYSIS

In the simulated connection test (Fig. 1), the major contribution of the flanges to the load-carrying capacity of the web panel may be described by two types of action. The first of these is that the flanges act as bearing plates to spread the concentrated beam flange force over some large area such as the value $(t_b + 5k)$ used in developing Eq. 1. The second is that the flanges serve to provide simply supported edge conditions for the web panel, because of the very high bending stiffness of the flange in the plane of the flange. There is an elastic solution reported in Ref. 4 for the buckling of a simply supported long plate compressed by two equal and opposite forces. If the slenderness ratio is taken to be the web depth between k lines, d_c, divided by the web thickness, w, the buckling load of the web panel is, in the usual notation

$$P_{cr} = \frac{4\pi D}{d_c} \tag{3}$$

where

$$D = \frac{E\,w^3}{12(1-\nu^2)} \tag{4}$$

From observations of the test results in the present tests, it appears that, far more than in the elastic range, the plastic behavior of the web plate is primarily a local matter and does not depend too much upon geometry and loading of the entire column. Therefore, it appears reasonably justified to assume that the concentrated load acts only across an effective width, and this width

forms a square panel, d_c by d_c. Thus the critical
buckling stress becomes

$$\sigma_{cr} = \frac{P_{cr}}{d_c w} = \frac{\pi E}{3(1-\nu^2)} \frac{1}{(d_c/w)^2} \tag{5}$$

valid for

$$\sigma_{cr} \leq \sigma_y \tag{6}$$

Using the typical set of values for steels:
E = 29,000 ksi and ν = 0.3, Eq. 5 reduces to

$$\sigma_{cr} = \frac{33,400}{(d_c/w)^2} \tag{7}$$

valid for

$$\frac{d_c}{w} \leq \frac{183}{\sqrt{\sigma_y}} \tag{8}$$

This limiting value of d_c/w comes very close to
providing us with the formula found in the AISC Specifica-
tions (See Eq. 2)

$$\frac{d_c}{w} = \frac{180}{\sqrt{\sigma_y}} \tag{9}$$

Using Eq. 9, Eq. 7 can be reduced to the non-
dimensional form

$$\frac{\sigma_{cr}}{\sigma_y} = \frac{1}{\left[\dfrac{d_c/w}{(d_c/w)_a}\right]^2} \tag{10}$$

Comparison with Test Results will be discussed later.

3. DESCRIPTION OF TESTS

3.1 Test Program

Nine tests were performed making use of available material. The first two were not fully instrumented. They did, however, provide data points for analysis of the behavior. Tests 3 through 9 comprise the group whose load deflection curves are presented.

The two most important variables are the yield strength and the d_c/w ratio. The allowable d_c/w ratio is calculated from AISC Formula (1.15-2) (Eq. 9). Table 1 summarizes the d_c/w ratios tested. It also lists the d'/w ratios, where d' is the distance between column flanges.

The first two test specimens, W-3 and W-4, were A514 steel, with d_c/w ratios 44% and 71% greater than allowable. The next two specimens, W-5 and W-6, were of A36 steel, with d_c/w ratios 37% and 4% greater than allowable. Test W-7 was of an A440 specimen almost exactly at the allowable slenderness ratio, followed by specimen W-8, an 8-inch deep heavy section of A36 steel, with a slenderness ratio only one-third of allowable. The last test, W-9, was a W12 x 120 A514 specimen.

Table 2 summarizes the handbook and the measured properties of all test specimens.

3.2 Test Procedures

A test set-up was devised which permits rapid testing of specimens. It is basically the same one used by Graham et al.[1], but with more complete instrumentation. The test set-up is shown in Figs. 1 and 2. In this simulation test, a column is placed horizontally between the loading platens of the testing machine and compressed by two steel bars placed in the same vertical plane on the top and bottom surfaces of the column. The bar was tack-welded to the column flange to simulate a beam flange framing in. All the specimens except one were tested in the Rhicle 800 kip mechanical machine at Fritz Laboratory. The largest specimen required the 5000 kip hydraulic machine.

The instrumentation consisted of dial gages to monitor the deflection in the direction of the applied load (which is plotted in Figs. 3 through 6) and another gage to monitor the lateral deflection of column web. This lateral deflection indicated the onset of buckling.

Two tensile specimens were cut from each specimen, in the orientation shown in Fig. 1, in accordance with ASTM standards. Although the principal loading direction is transverse, the standards call for specimens taken in the longitudinal direction.

4. RESULTS

4.1 Load-Deflection Behavior

The load deflection diagrams are presented in Figs. 3 to 6. Figures 3 and 4 show specimens whose d_c/w ratio were greater than or close to allowable. Note that ultimate load is followed by unloading. Fig. 5 shows the diagram for three specimens with three different d_c/w ratios: greater than, close to, and less than allowable. There was an unloading for the specimen with safe d_c/w ratio but it occurred at much greater values of deflection. All three specimens in Fig. 5 were of steel with 36 ksi yield point. Similar curves for specimens with a 100 ksi yield point are shown in Fig. 6. It should be noted that tests 8 and 9 were of heavy column sections.

Comparing tests 3,4,5,6, and 7 with test 8 indicates that stockier sections do not have as steep an unloading curve as the slender ones, nor do they reach ultimate load at as small a deflection. This is partly due to the slenderness of column web. A great deal of difference may be attributed to the contribution of the flanges. The heavier specimens had considerably thicker flanges.

4.2 Yield Pattern

The yield stress pattern at ultimate load varied from test to test. Figure 7 shows an almost perfectly rectangular distribution of yielding at the ultimate load

of test W-4. The yielded width is 5 inches. A dissimilar pattern is found in Fig. 8. It shows the yield pattern at the ultimate load of test W-5, where the yielded width at the toe of the fillet is 6 inches. Another type of yield pattern is presented in Fig. 9, from test W-7, where the yielded width was 10 inches.

Ultimate load was marked by the onset of large lateral deflections in all tests. The yield pattern immediately spread for great distances as the test was pursued into the unloading region. Two examples of the resulting yield patterns are shown in Figs. 10 and 11. Table 3 presents the ultimate load and the predicted load for each test.

4.3 Analysis

All of the earlier data, from Graham et al.[3] (summarized in Table 4), was combined with this data and plotted in Fig. 12. The non-dimensionalized load, $P/(t_b + 5k)w\sigma_y$, is plotted against the normalized slenderness ratio.

Figure 12 shows that the prediction of $(t_b + 5k)w\sigma_y$ is conservative in all cases but can be anywhere between 50 percent and 70 percent of the observed load in the safe region.

The specimens whose d_c/w ratios are greater than or close to allowable are plotted in Fig. 13, with

an ordinate of $\sigma = P/d_c w$. The solid curved line (Eq.7)

is the prediction by the theoretical analysis developed

in Section 2. It is seen that except for Tests 3 and 4,

the theoretical curve is in good agreement with test

results. Tests 3 and 4 are seen to develop a buckling

strength far in excess of that indicated by the theoreti-

cal curve. This may be expected because Tests 3 and 4

are specimens of high strength steel with d_c/w ratios much

greater than allowable. In such case, buckling may take

place only after small areas of inelastic strain developed

near the immediate areas of the concentrated forces, and

the web plate remains essentially in the elastic range.

The effective width concept, upon which the inelastic

buckling stress was calculated, does not apply, because

the elastic behavior of the web plate is no longer a local

matter but depends upon the geometry and loading of the

entire web plate.

In the elastic buckling case, the column flanges

appear to provide some additional moment restraint for

the web plate, because of the very limited local yielding

at the depth of the base of the column flange fillet

(k-depth).   Timoshenko shows that the buckling load

of the clamped long plate is exactly twice the value given

by Eq. 3 [4]. For Tests 3 and 4, these buckling loads

are found to be 328 kips and 274 kips, which give 253 kips

and 260 kips as the upper limits for the test values

respectively. Thus the previous discussions on the plate

edge conditions is reasonable in such cases.

All of the earlier data from Ref. 3, was
combined with present data and plotted in Fig. 14. The
non-dimensionalized load, σ/σ_y, is plotted against the
normalized slenderness ratio. The straight line is
$\sigma=\sigma_y$ and the curved line (Eq. 10) is the theoretical
prediction. The theoretical curve fits well in the slender
range, where d_c/w is greater than allowable.

Figure 15 substitutes, d', the web depth
between flanges, for d_c in Fig. 14. It can be seen that
the agreement is comparable to that of Fig. 14.

4.4 Deformation Capacity

When the column web has the requisite strength
the desired rotation capacity of the connection is supplied
jointly by the column web and the end portions of the
beam. A rough idea of deformation capacity of the column
web can be estimated by setting θ, the hinge angle rota-
tion, equal to Δ, the measured deformation, divided by
the depth of the beam, d_b. For $\Delta_{ult} \sim 0.2$ to 0.5 inches
(see Tests 3 to 7), θ_{ult} is in the range of necessary
rotation (this varies from structure to structure). It
is possible that such a hinge will not deform sufficiently
to re-distribute its moments. A safe section (Tests 8
and 9) probably will develop sufficient rotation.

5. SUMMARY AND CONCLUSIONS

(1) The two most important variables in the present study are the yield strength and the web depth-to-web thickness ratio. With regard to strength and stability, the results show that the present AISC Specifications are conservative for all grades of steel.

(2) It is found that strength and stability of column web could be more accurately predicted by the curves shown in Fig. 14 or 15. It should be kept in mind, however, that if a slender shape is used, the danger of unloading as well as the deformation capacity must be considered.

6. ACKNOWLEDGEMENTS

7. <u>REFERENCES</u>

1. AISC Specification for the Design, Fabrication, and
        Erection of Structural Steel for Buildings,
        American Institute of Steel Construction,
        February, 1969.

2. ASCE Manuals of Engineering Practice No. 41, Commentary
        on Plastic Design in Steel, the Welding Research
        Council and the American Society of Civil Engi-
        neers, 1961 (Revision to Appear in 1970).

3. Graham, J. D., Sherbourne, A. N., Khabbaz, R. N., and
        Jensen, C. D., WELDED INTERIOR BEAM-TO-COLUMN
        CONNECTIONS, AISC Publication, Fritz Engineering
        Laboratory Report No. 233.15, 1959. Also,
        Bulletin No. 63, WELDING RESEARCH COUNCIL, New
        York, August, 1960.

4. Timoshenko, S. P. and Gere, J. M.
        THEORY OF ELASTIC STABILITY, 2nd edition,
        McGraw-Hill, New York, 1961.

8.   NOMENCLATURE

A_f = area of one flange (of the beam framing in);

C_1 = ratio of the beam flange yield stress to the column yield stress;

d_c = column web depth between column k-lines or between toes of fillets;

d_b = depth of beam;

d' = distance between column flanges, Fig. 1;

E = Young's modulus of elasticity;

k = distance from outer face of flange to web toe of fillet, Fig. 1;

P = concentrated load;

t_b = thickness of the beam flange;

w = column web thickness;

σ = normal stress;

σ_y = yield stress in ksi;

ν = Poisson's ratio;

δ = lateral displacement, Fig. 1;

Δ = vertical displacement, Fig. 1;

θ = hinge angle rotation;

TABLE 1

TEST PROGRAM

Test No.	Section	Actual σ_y ksi	Allowable d_c/w $= \dfrac{180}{\sqrt{\sigma_y}}$	Actual d_c/w	$\dfrac{d_c/w}{(d_c/w)_a}$	d'/w	$\dfrac{d'/w}{(d_c/w)_a}$
3	W10x39	121.9	16.4	23.7	1.44	26.4	1.61
4	W12x45	118.2	16.7	28.6	1.71	31.8	1.90
5	W12x31	39.8	28.6	39.2	1.37	41.6	1.45
6	W10x29	41.6	27.9	28.9	1.04	30.2	1.08
7	W10x54	57.8	23.7	21.2	0.89	23.3	0.99
8	W 8x67	30.9	32.4	11.5	0.36	12.5	0.39
9	W12x120	97.7	18.2	14.2	0.78	15.6	0.86

TABLE 2

SECTION PROPERTIES

Test No.	Section	Handbook					Measured				
		σ_y ksi	d_c in.	w in.	k in.	d' in.	σ_y ksi	d_c in.	w in.	k in.	d' in.
3	W10x39	100	7.88	0.318	1.06	8.88	121.9	8.15	0.344	0.91	9.05
4	W12x45	100	9.75	0.336	1.19	10.91	118.2	9.87	0.344	1.11	10.93
5	W12x31	36	10.38	0.265	0.88	11.16	39.8	10.59	0.270	0.70	11.22
6	W10x29	36	8.50	0.289	0.88	9.22	41.6	8.91	0.308	0.73	9.32
7	W10x54	50	7.87	0.368	1.13	8.88	57.8	8.05	0.380	1.02	8.86
8	W 8x67	36	6.38	0.575	1.31	7.13	30.9	6.60	0.575	1.22	7.21
9	W12x120	100	9.75	0.710	1.69	10.91	97.7	9.95	0.700	1.57	10.96

TABLE 3

TEST RESULTS

Test No.	t_b in.	Computed $(t_b + 5k) w\sigma_y$ kip	Test P_{ult} kip	$\dfrac{P_{ult}}{d_c\, w\sigma_y}$	$\dfrac{P_{ult}}{d'\, w\sigma_y}$
3	0.50	212	253	0.74	0.67
4	0.50	246	260	0.65	0.58
5	0.50	43	61	0.54	0.51
6	0.50	53	90	0.79	0.75
7	0.50	123	215	1.20	1.10
8	0.93	125	250	2.14	1.95
9	1.11	612	980	1.45	1.31

TABLE 4

Test results reported by Graham, Sherbourne, Khabbaz and Jensen (see Ref. 3)

Test No.	Section	t_b in.	Actual σ_y ksi	Allowable $\frac{d_c}{w} = \frac{180}{\sqrt{\sigma_y}}$	Actual $\frac{d_c}{w}$	$\frac{d'}{w}$	Computed $(t_b + 5k)w\sigma_y$ kip	Test P_{ult} kip	$\frac{P_{ult}}{d_c\, w\sigma_y}$	$\frac{P_{ult}}{d'\, w\sigma_y}$
E 1	W12x40	0.5	40.2	28.4	33.20	37.1	81.6	102.5	0.89	0.79
E14	W 8x48	0.5	34.4	30.7	15.70	18.0	89.8	137.0	1.54	1.37
E15	W 8x58	0.5	36.2	29.9	12.50	14.0	119.1	202.5	1.72	1.53
E16	W10x66	0.5	40.0	28.5	17.23	19.4	143.9	175.7	1.22	1.08
E17	W10x72	0.5	35.0	30.4	15.40	17.4	129.6	190.0	1.35	1.19
E18	W12x65	0.5	37.2	29.6	25.00	28.0	93.2	143.0	1.01	0.90
E19	W12x85	0.5	37.8	29.3	19.69	22.0	151.2	247.5	1.35	1.21
E20	W14x61	0.5	36.2	29.9	30.10	33.4	110.0	137.5	0.88	0.79
E21	W14x68	0.5	38.3	29.1	27.20	30.2	132.1	164.0	0.90	0.81
E22	W14x84	0.5	39.3	28.7	25.22	28.0	133.6	221.0	1.09	0.98
E23	W14x104	0.5	38.5	29.0	23.00	25.5	160.0	250.0	1.15	1.03
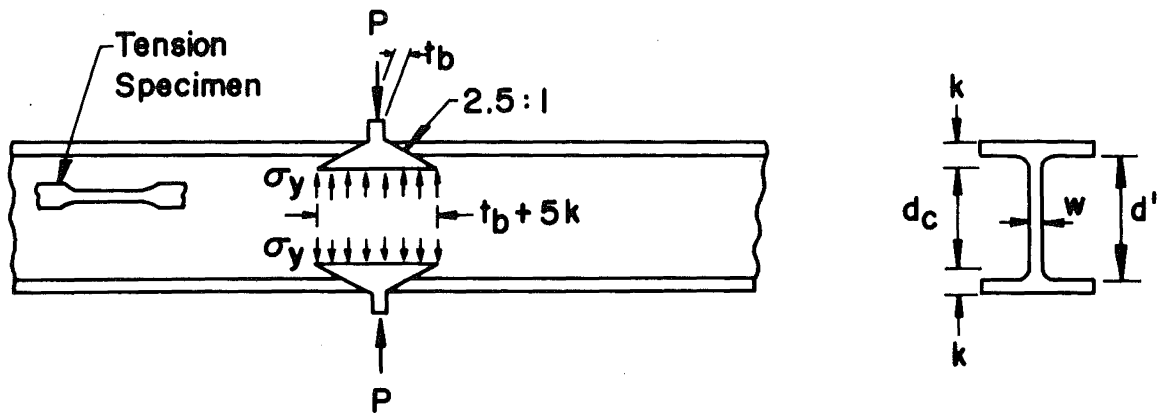
Fig. 1   Simulation of the Compression Region
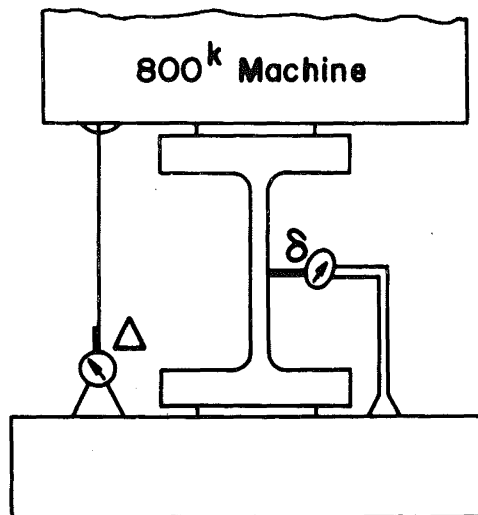
Fig. 2   Test Set-up
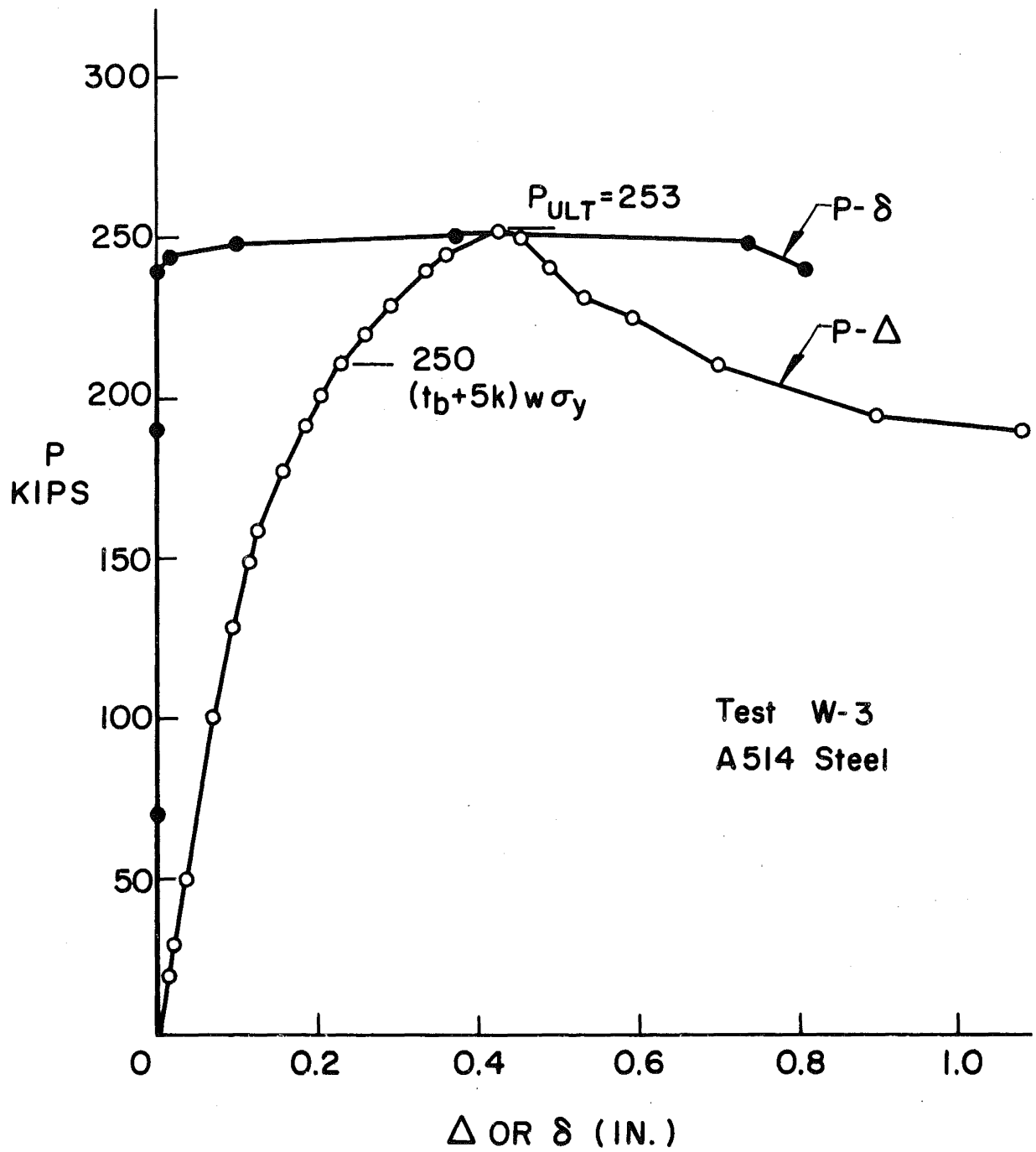
Fig. 3 Load-Deflection Curves
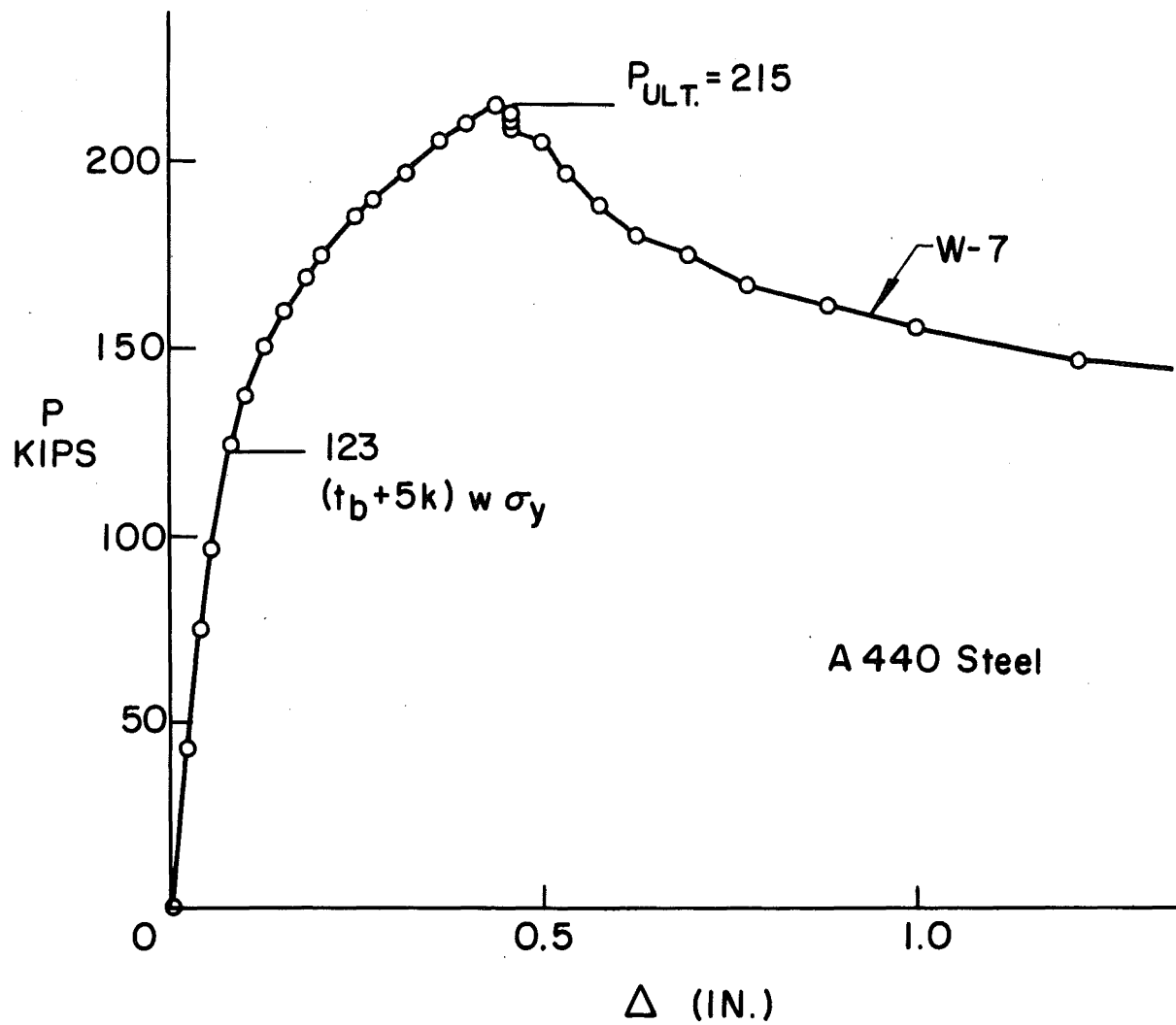
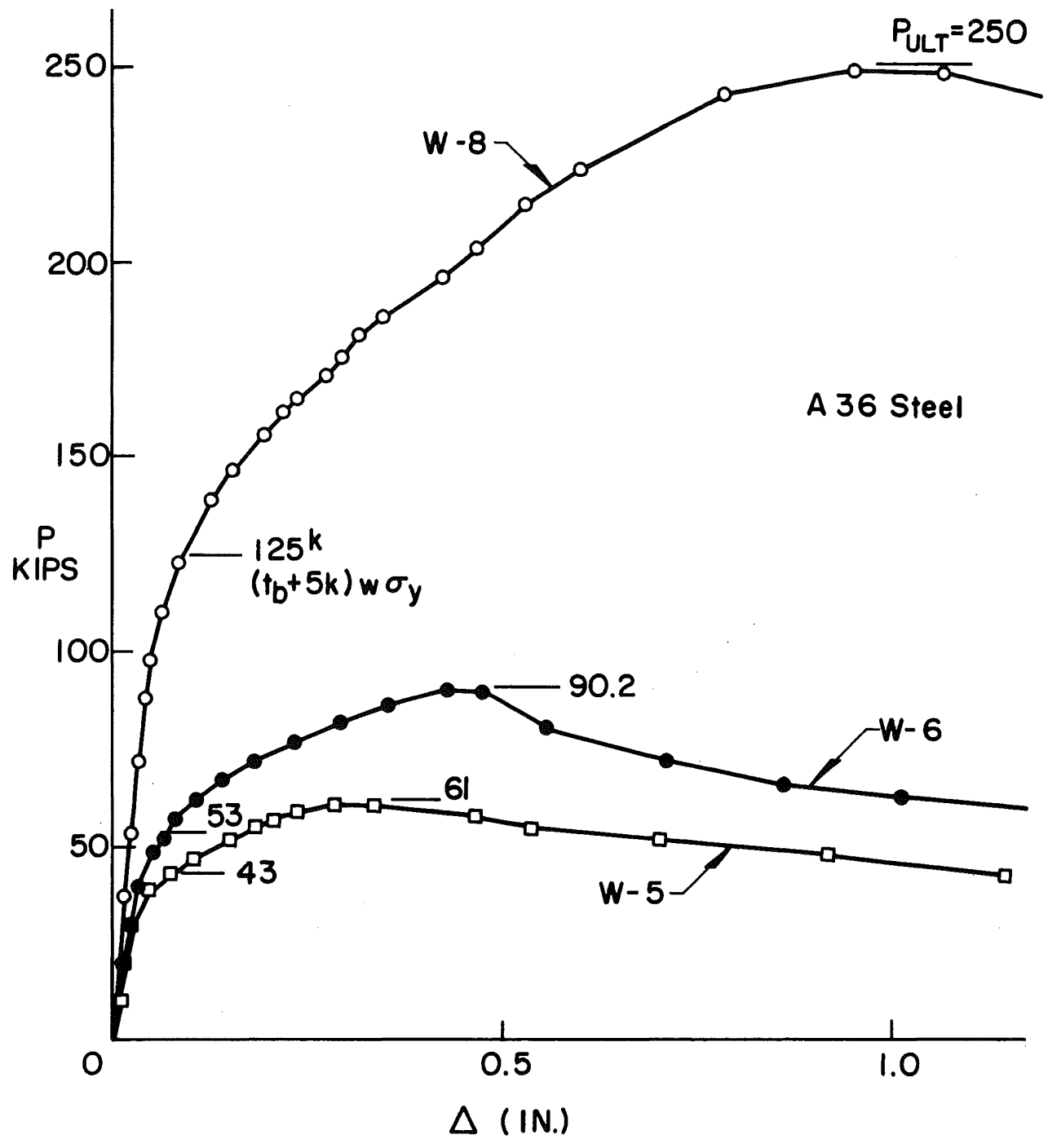Fig. 4 Load-Deflection Curve

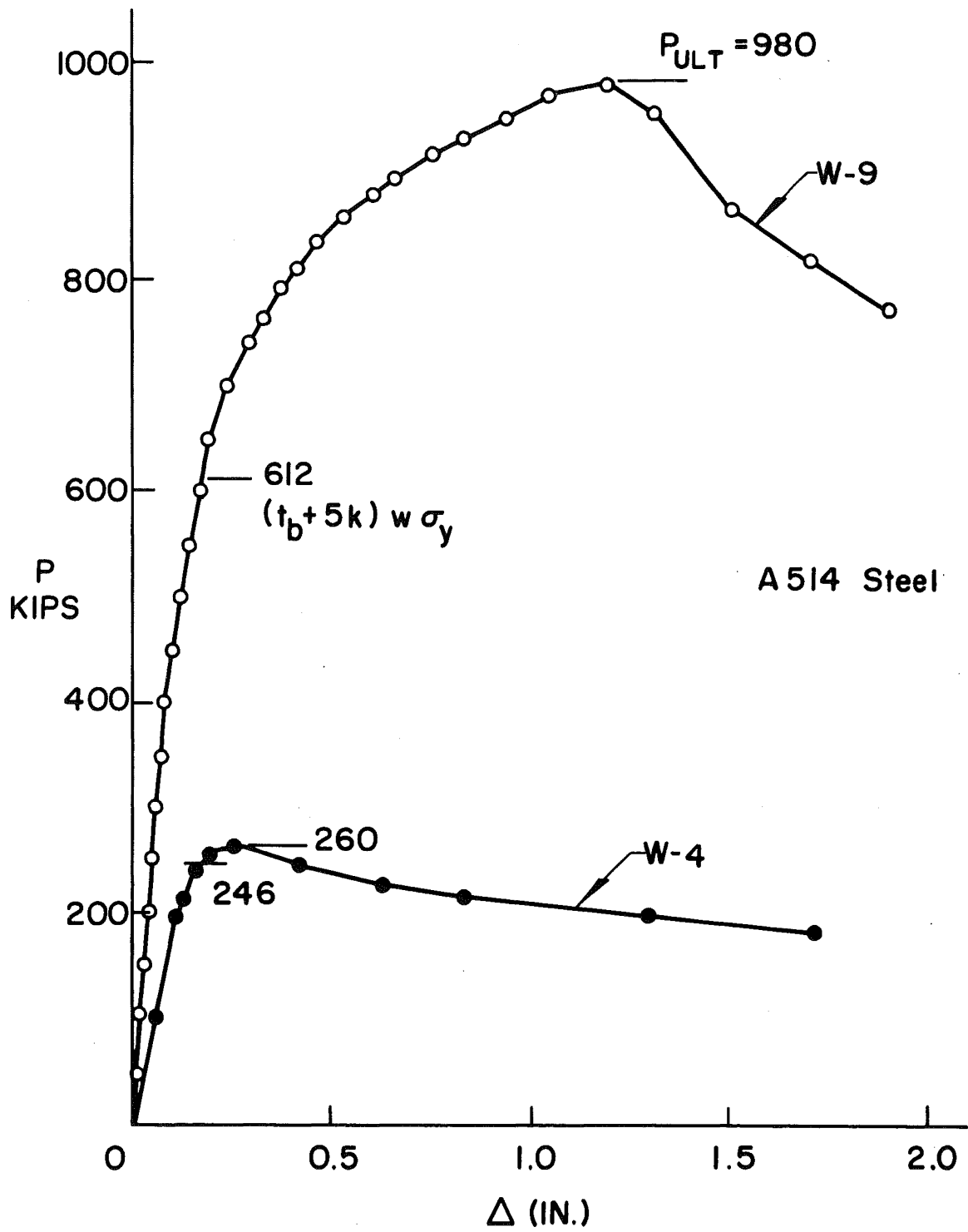Fig. 5 Load-Deflection Curves

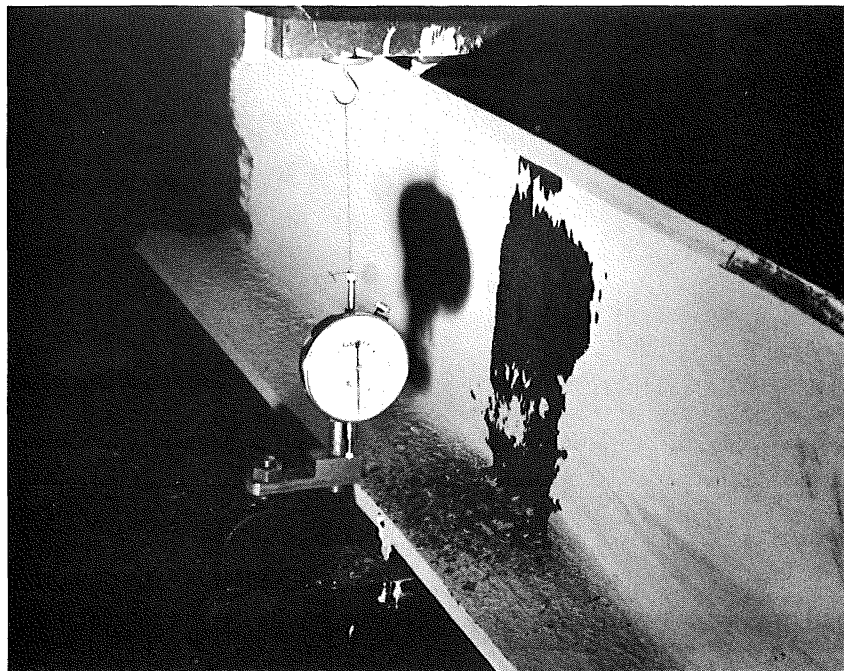Fig. 6   Load-Deflection Curves

Fig. 7   Rectangular Distribution of Yielding
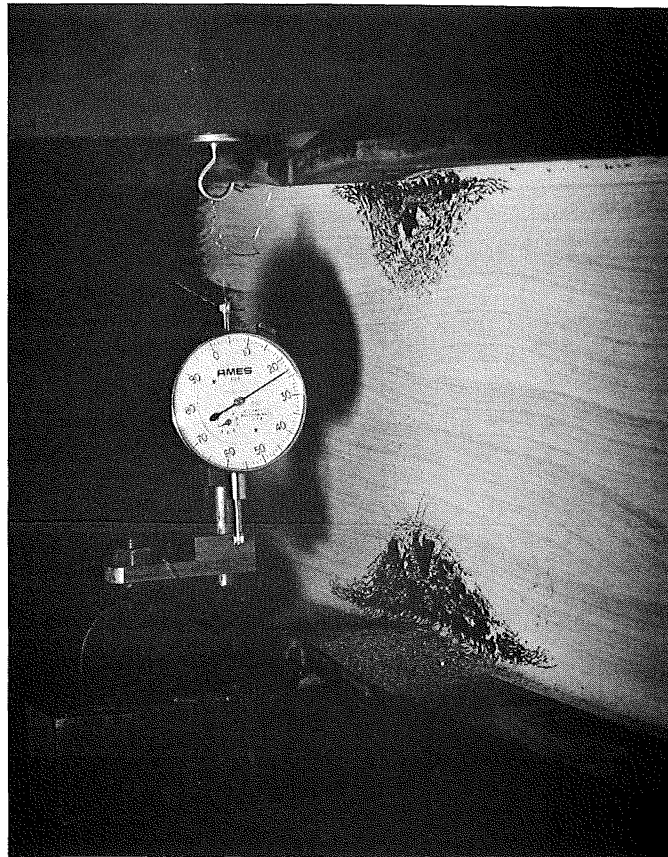
at the Ultimate Load of Test W-4

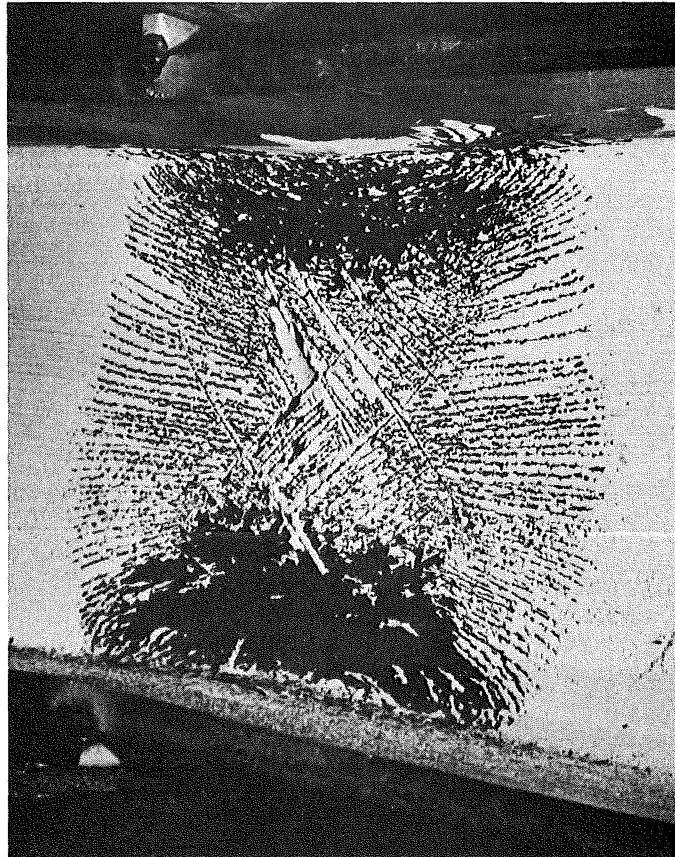Fig. 8 Yield Pattern at the Ultimate Load of Test W-5

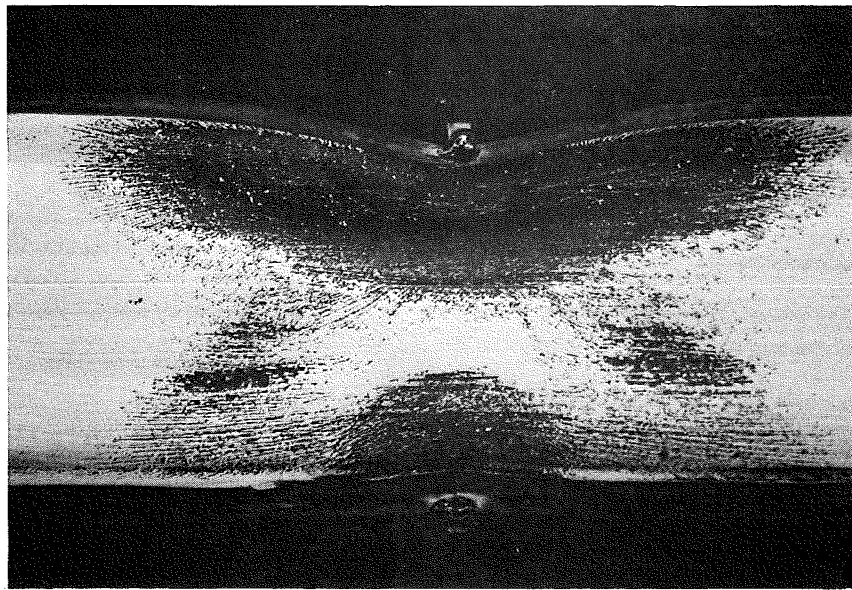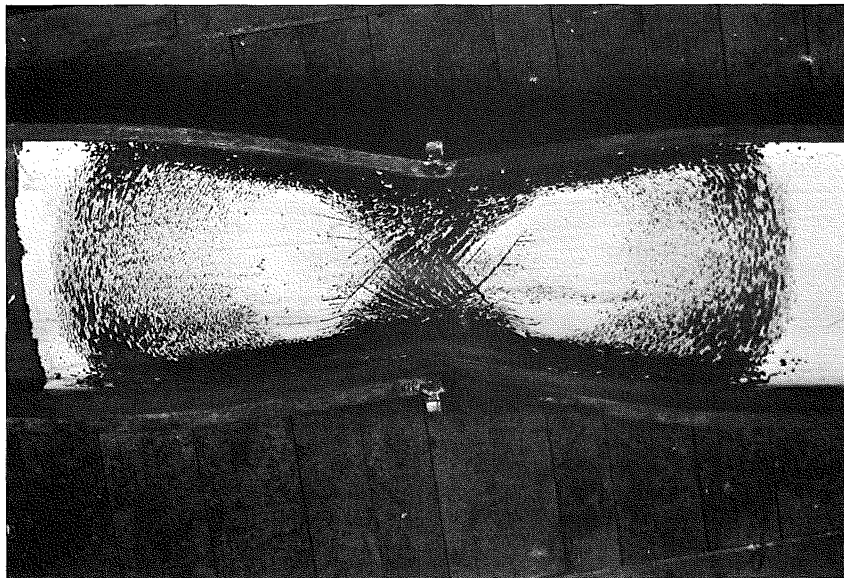Fig. 9 Yield Pattern at the Ultimate

Load of Test W-7

Fig. 10 Yield Pattern Immediately After the

Ultimate Load of Test W-7 was Reached

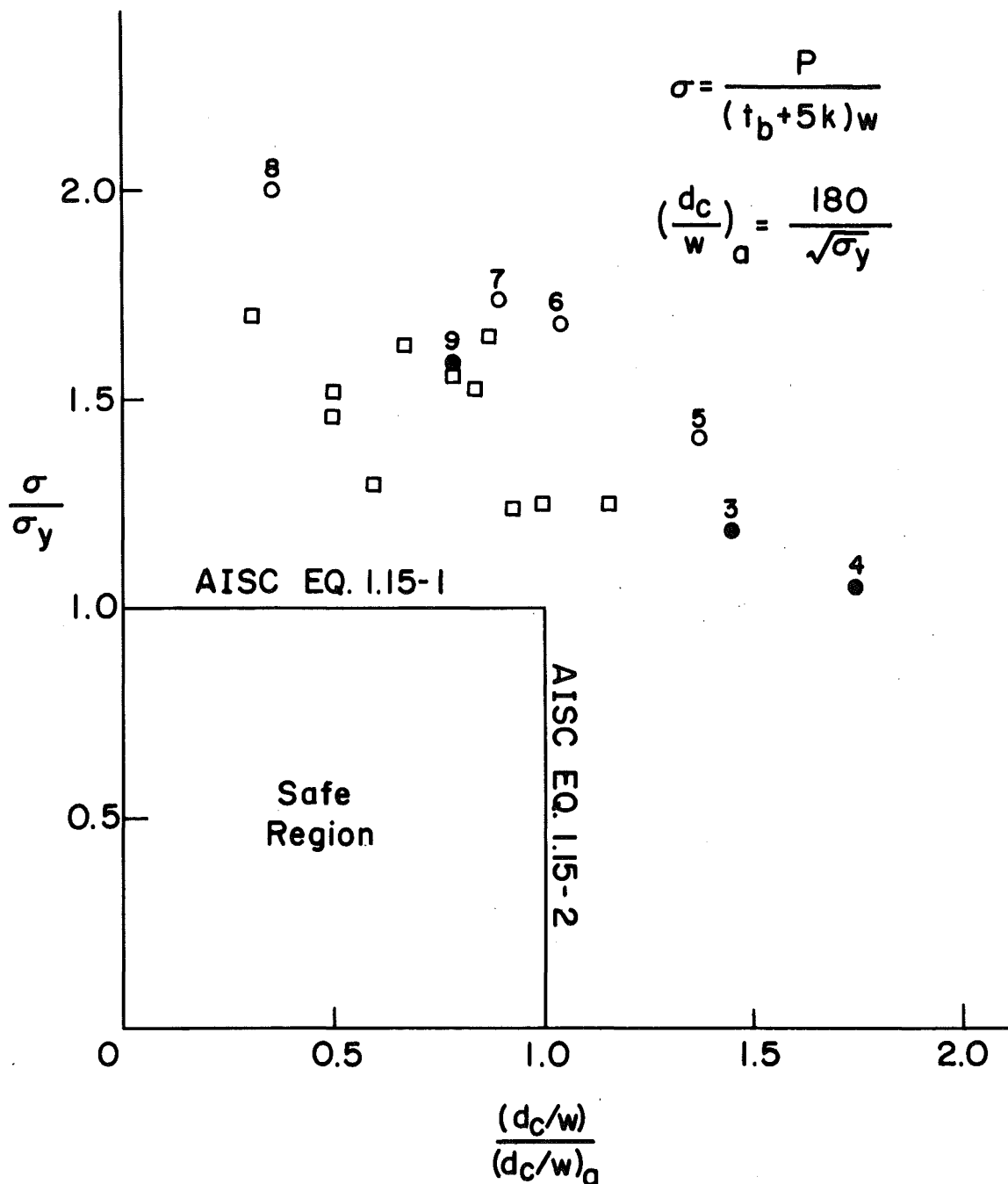Fig. 11   Yield Pattern at the End

of Test W-7

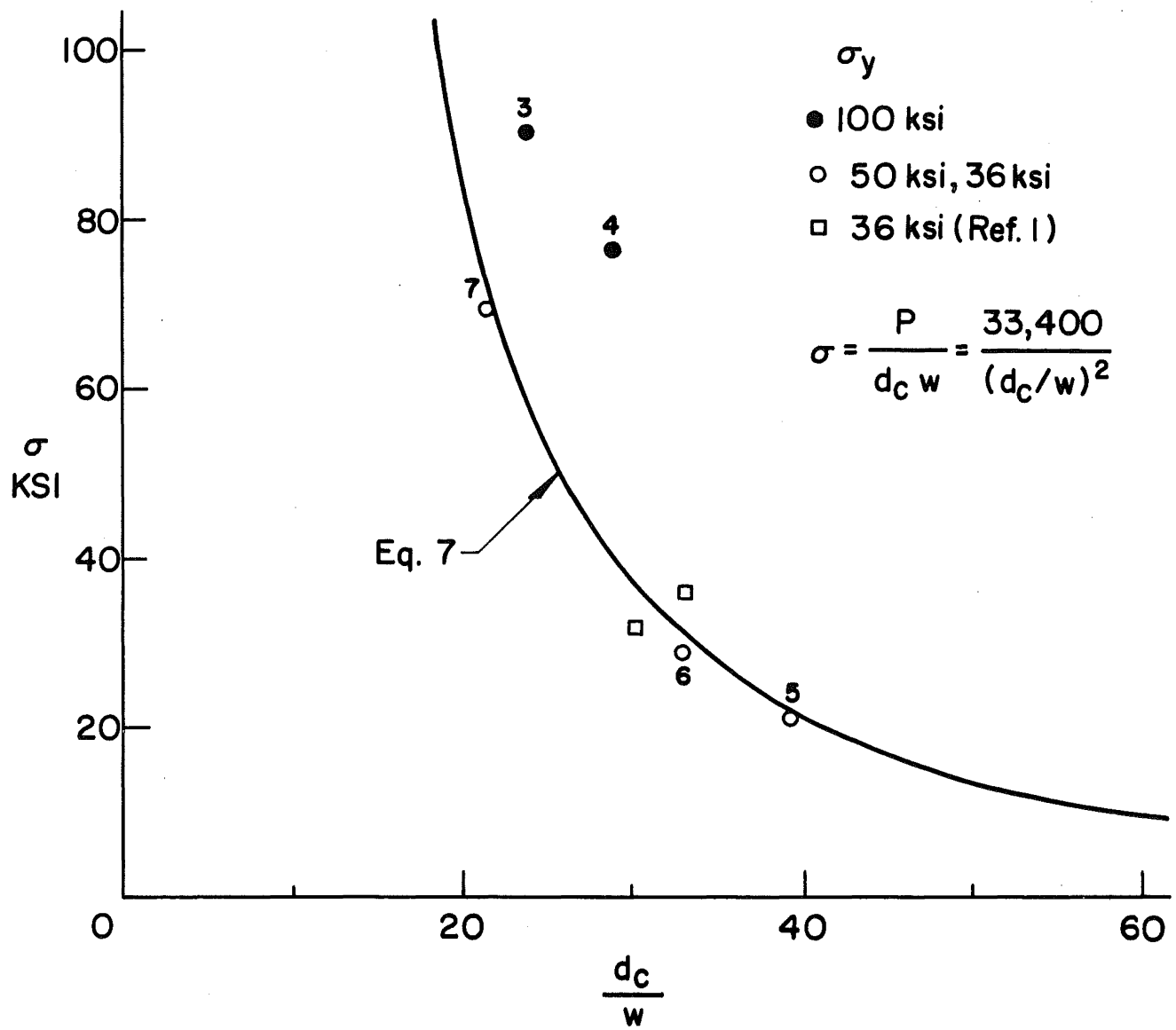Fig. 12   Comparison of Test Results

With AISC Formulas

$$\sigma_y$$

● 100 ksi

○ 50 ksi, 36 ksi

□ 36 ksi (Ref. 1)

$$\sigma = \frac{P}{d_c\,w} = \frac{33,400}{(d_c/w)^2}$$

Fig. 13 Comparison of Analytical Results with
Tests for Specimens with d_c/w Ratio
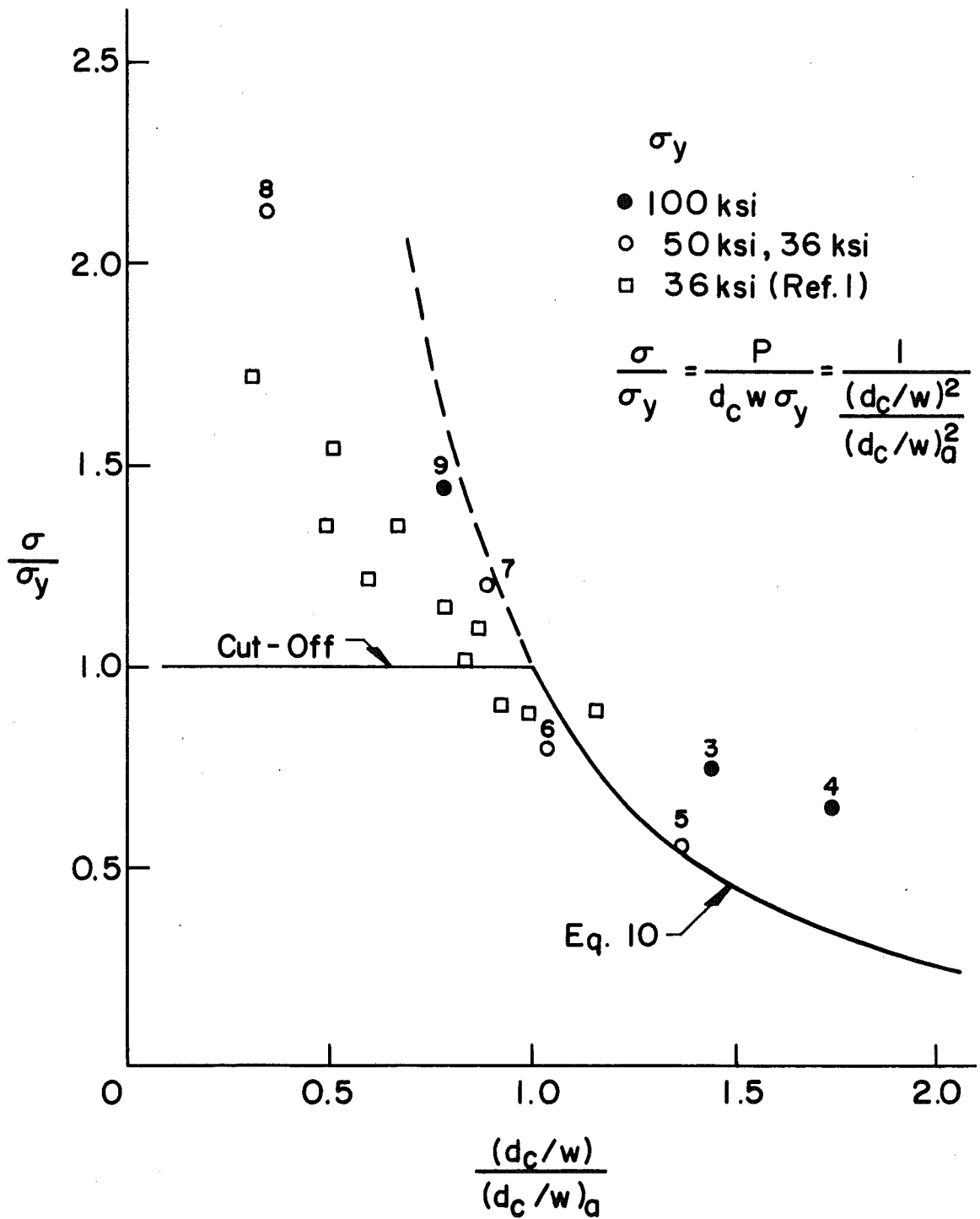Greater Than or Close to Allowable

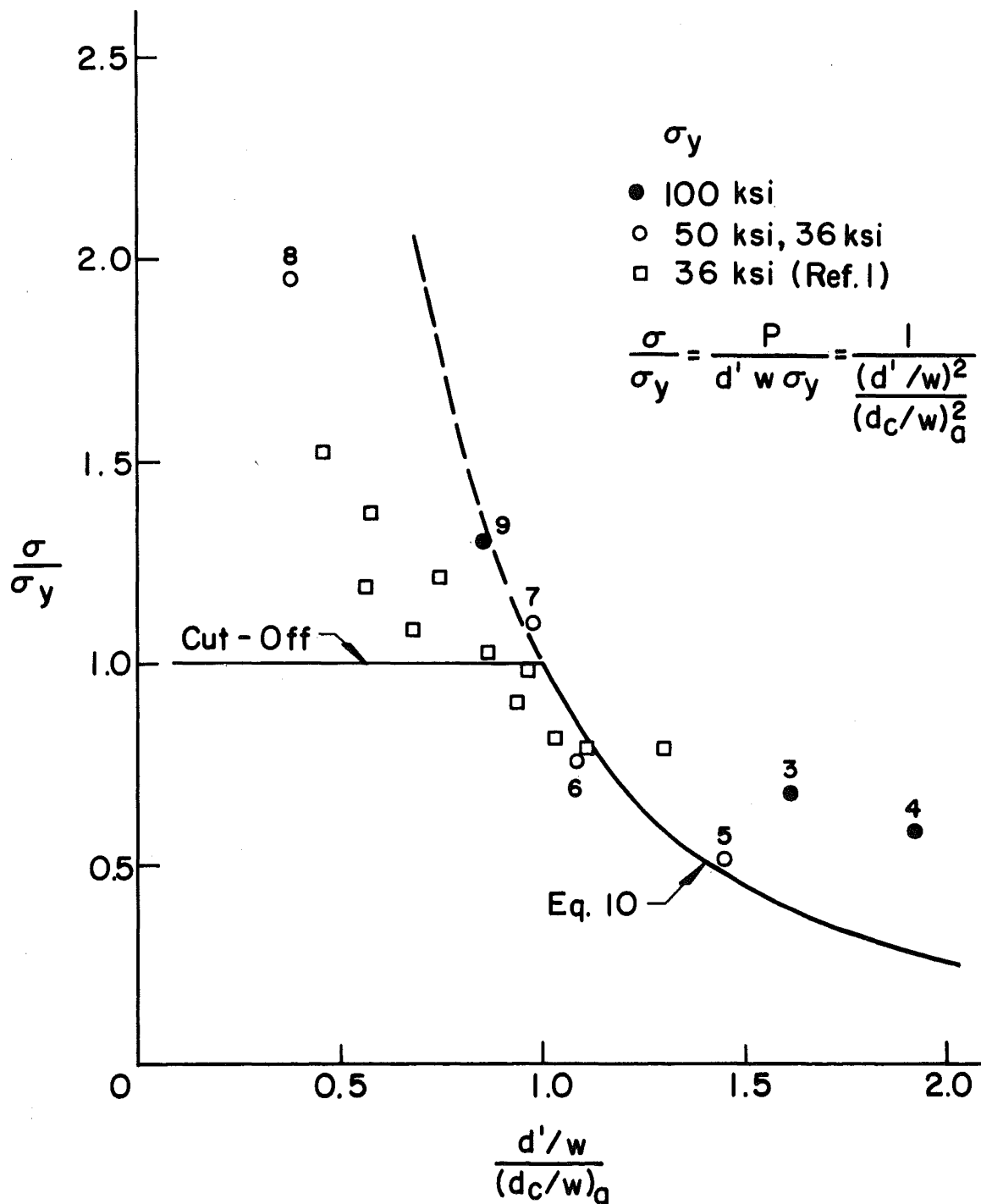Fig. 14 Comparison of Analytical Results

With Tests (For all $\dfrac{d_c}{w}$)

Fig. 15 Comparison of Analytical Results
With Tests (Note: using d'
instead of d_c in Fig. 14)